Supporting Information

N-doped Hierarchical Porous Carbon Derived from Bismuth Salts Decorated ZIF8 as a Highly Efficient Electrocatalysts for CO_2 Reduction

Pengfei Yao[ab], Tianyu Li[a], Yanling Qiu[a], Qiong Zheng[a], Huamin Zhang[a], Jingwang Yan[a], Xianfeng Li*[a]

[a] Division of Energy Storage, Dalian Institute of Chemical Physics, Chinese Academy of Sciences, 457 Zhongshan Road, Dalian 116023 (P.R. China), Email: lixianfeng@dicp.ac.cn,
[b] University of Chinese Academy of Sciences, Beijing 100049 (P.R. China).

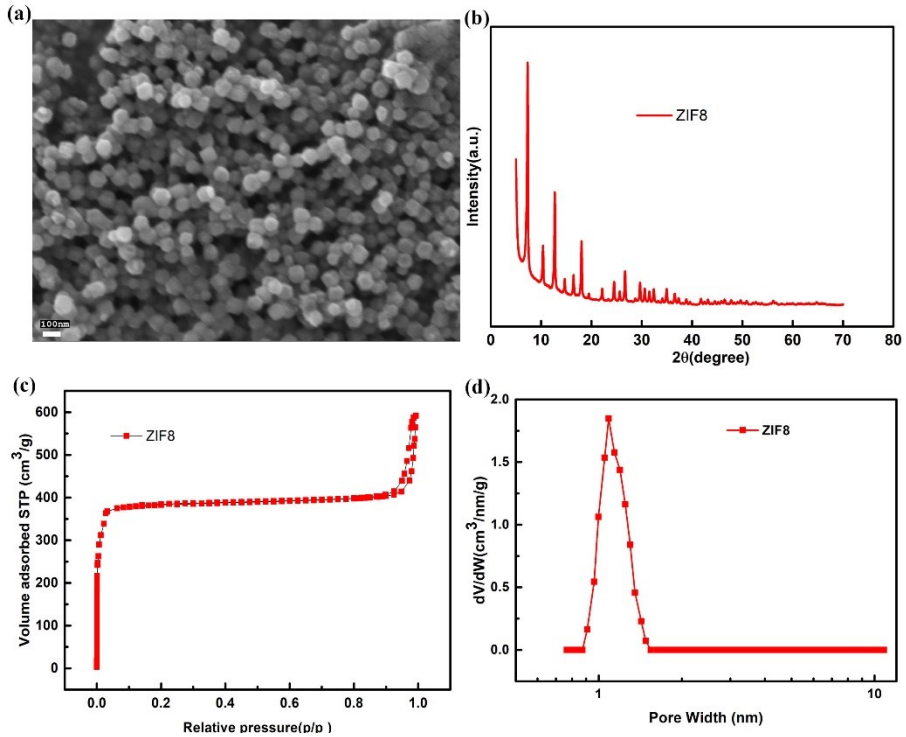

Figure S1. (a) SEM images of ZIF8 (b) The XRD of ZIF8 (c) Nitrogen adsorption–desorption isotherm of ZIF8 (d) Pore size distributions of ZIF8.

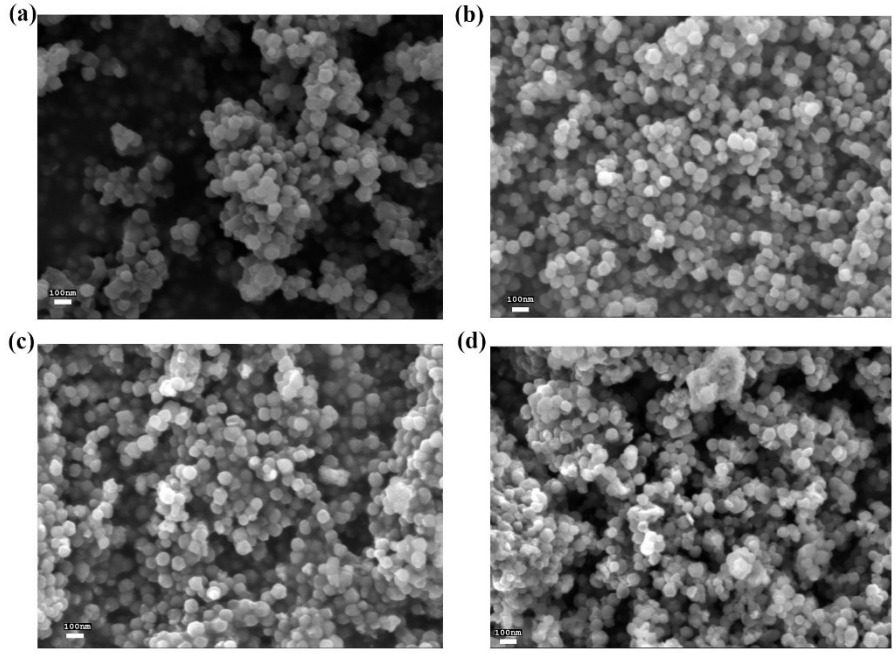

Figure S2. (a-d) SEM images of ZIF8, ZIF8-Bi, ZIF8-2Bi and ZIF8-4Bi.

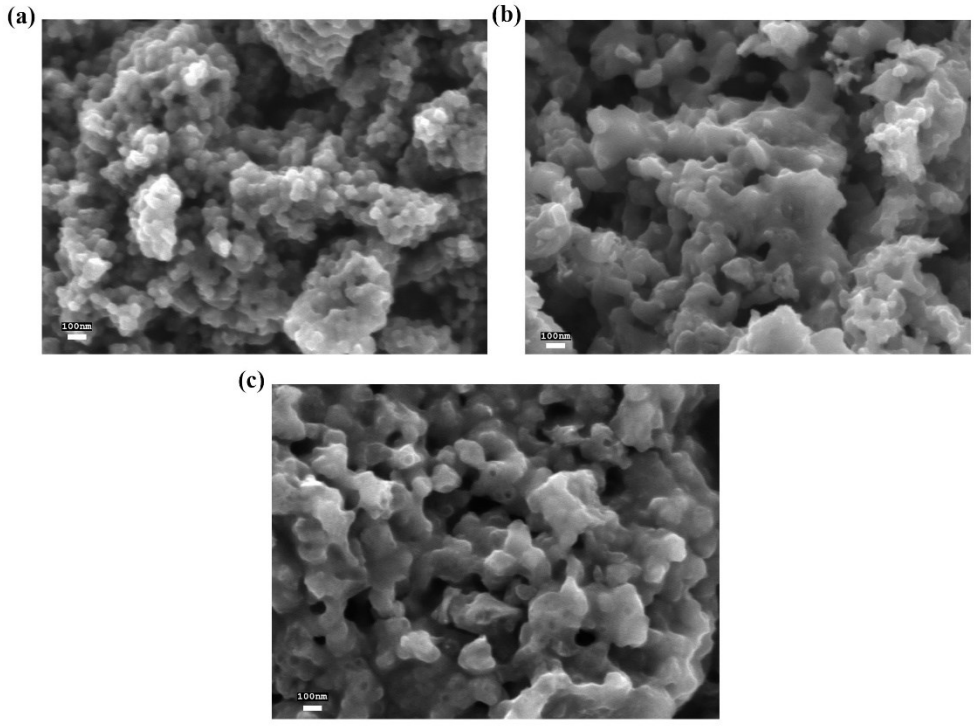

Figure S3. (a-c) SEM images of ZIF8-950, ZIF8-950-Bi, ZIF8-950-2Bi.

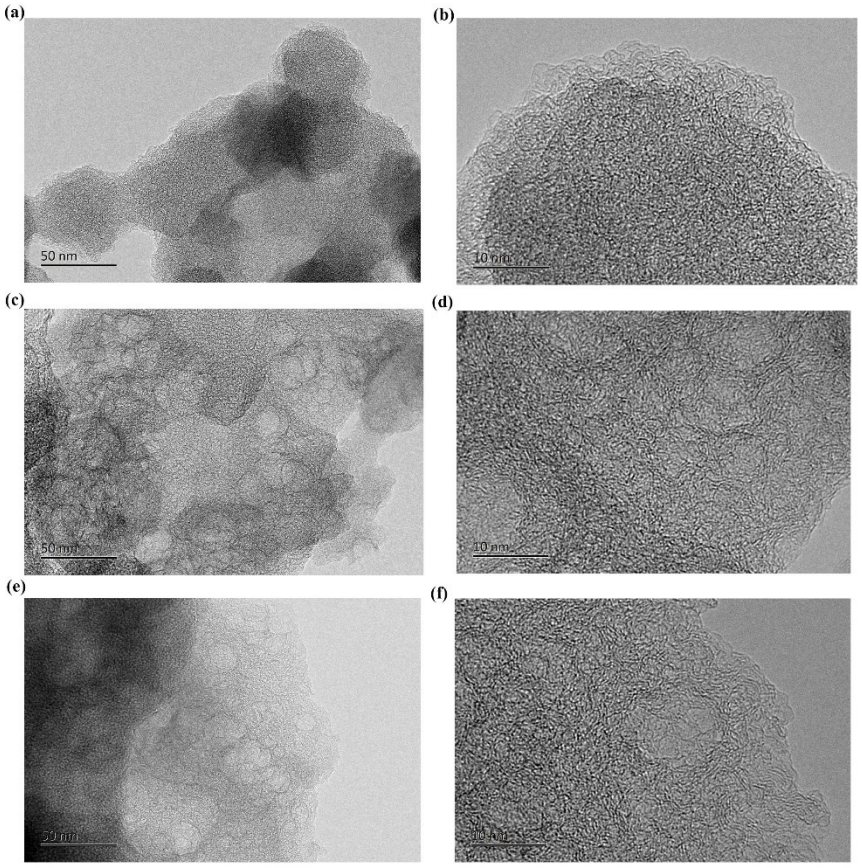

Figure S4. HTEM images of (a-b) ZIF8-950, (c-d) ZIF8-950-Bi, (e-f) ZIF8-950-2Bi.

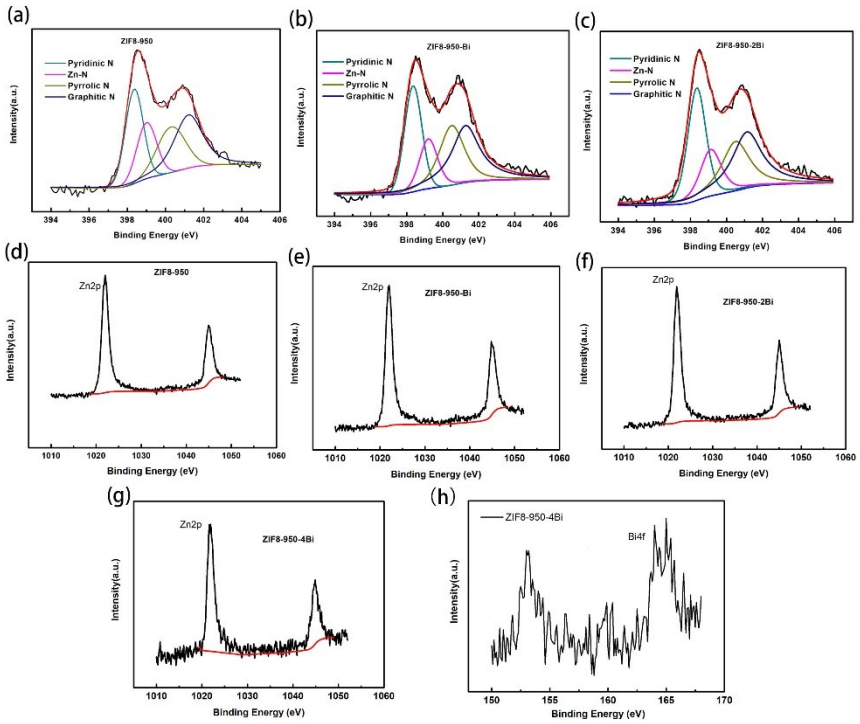

Figure S5. The XPS results for N 1s of (a) ZIF8-950, (b) ZIF8-950-Bi, (c) ZIF8-950-2Bi, (d-g) the XPS results for Zn2p of all samples, (h) the XPS results for Bi4f of ZIF8-950-4Bi.

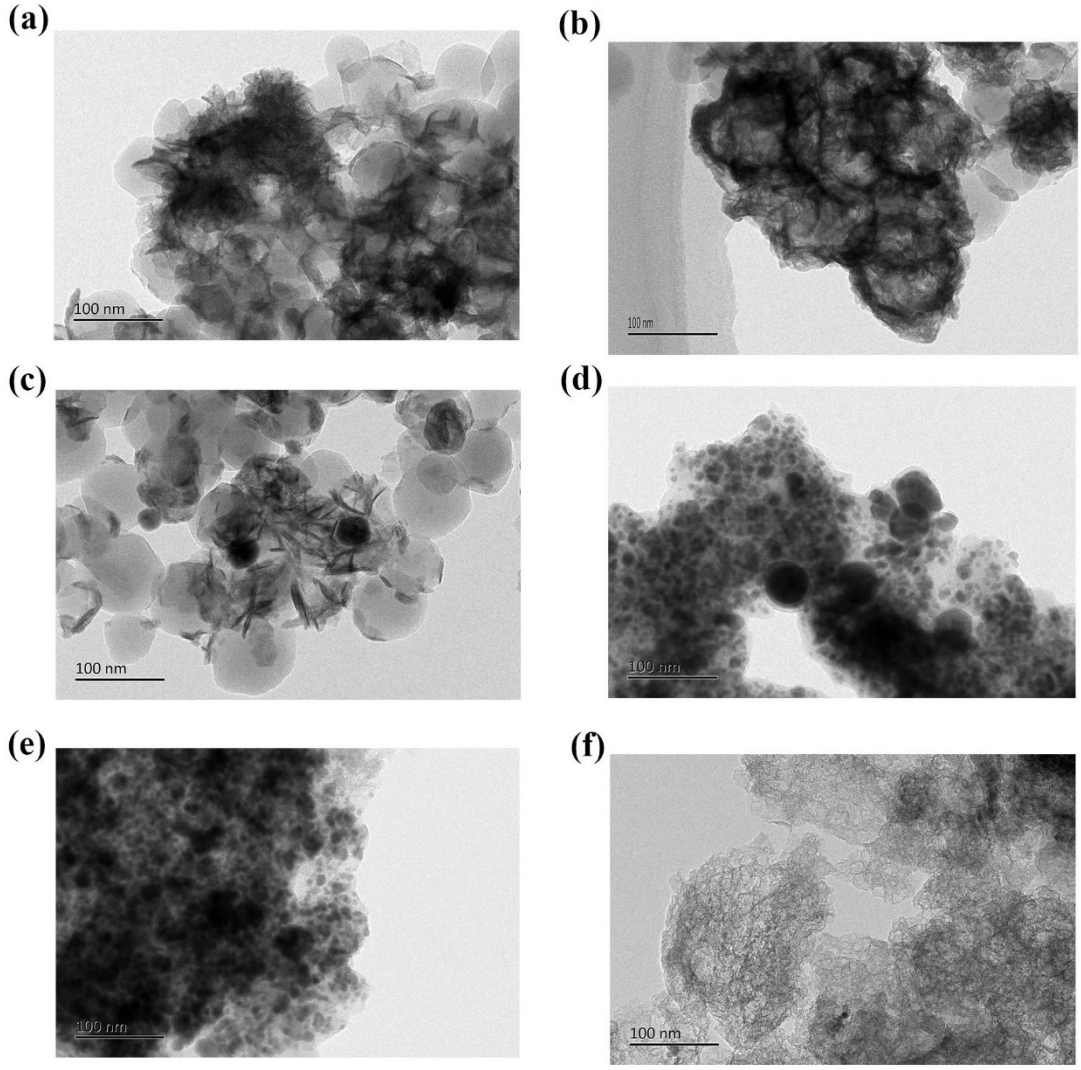

Figure S6. The HTEM of (a) ZIF8-4Bi, (b) ZIF8-250-4Bi, (c) ZIF8-350-4Bi, (d) ZIF8-550-4Bi, (e) ZIF8-750-4Bi, (f) ZIF8-950-4Bi

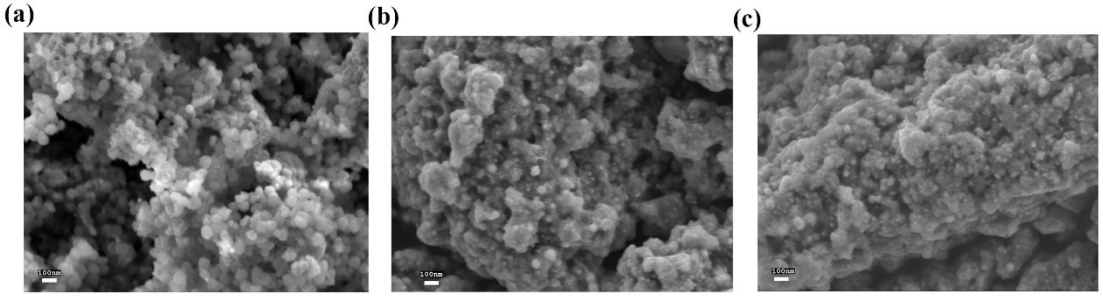

Figure S7. The SEM of (a) ZIF8-350-4Bi, (b) ZIF8-550-4Bi (c) ZIF8-750-4Bi

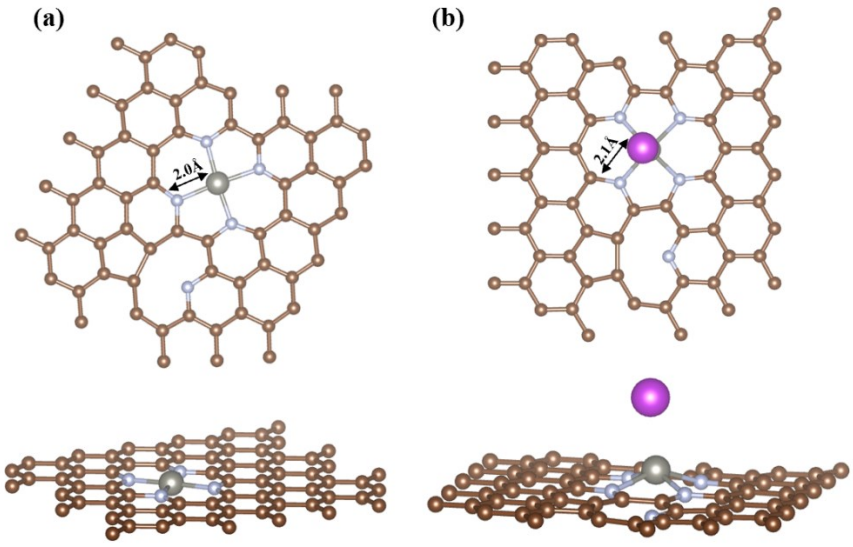

Figure S8. The most stable configurations of (a) Zn-N_4/C and (b) Bi modified Zn-N_4/C. The grey, white, brown and purple spheres are Ni, N, C, and Bi atoms.

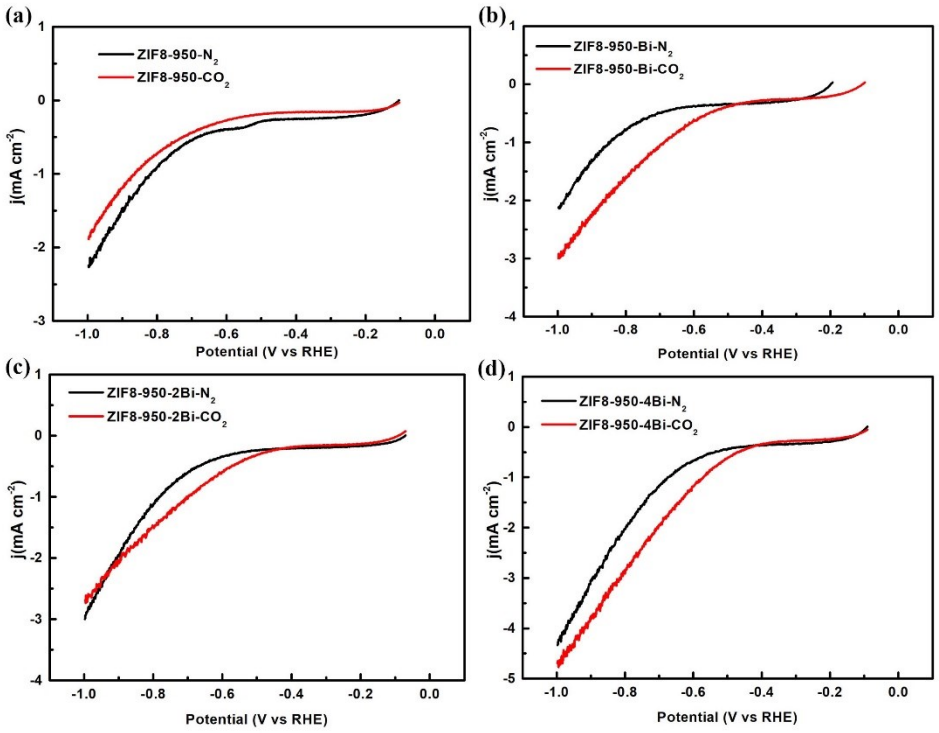

Figure S9. Linear sweep curves in the N_2-and CO_2-saturated 0.5 M $KHCO_3$ aqueous solution of (a) ZIF8-950, (b) ZIF8-950-Bi, (c) ZIF8-950-2Bi, (d) ZIF8-950-4Bi.

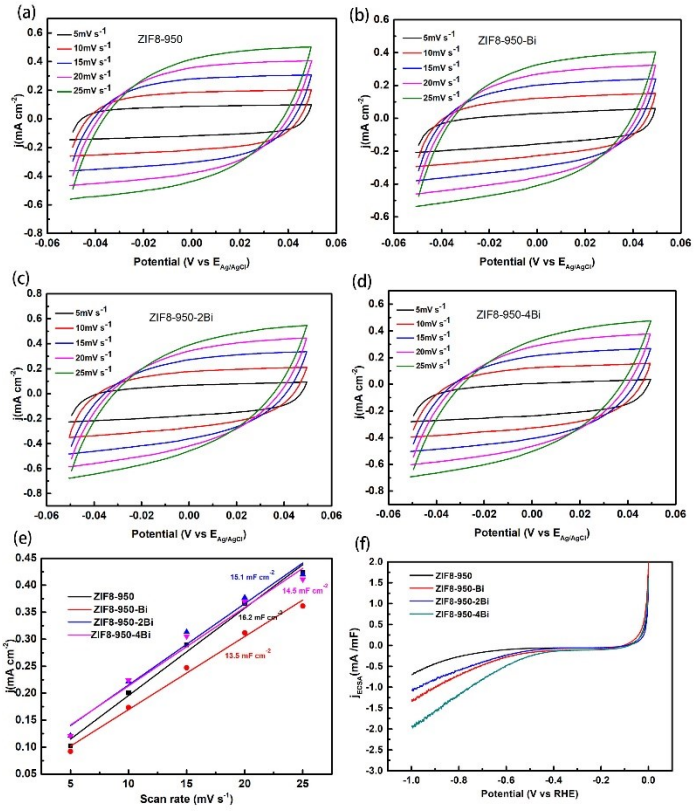

Figure S10. (a-d) Cyclic voltammograms of all samples with the potential range from 0.05 to -0.05 V (vs. $E_{Ag/AgCl}$) in a N_2-bubbled 0.5 M $KHCO_3$ electrolyte, (e) the ECSA for all samples. (f) the linear sweep curves of all the samples (normalized by ECSA).

DFT calculations

Computational methods: DFT calculations were carried out using the Vienna ab initio simulation package (VASP) [1] with the projector-augmented wave (PAW)[2] method. All calculations were based on the on the generalized gradient approximation (GGA)[3] method with Perdew-Burke-Ernzerhof (PBE)[4] functional for the exchange-correlation term. Van der Waals interaction was taken into account at DFT-D3[5, 6] with Becke-Jonson[7] damping algorithm. The plane wave cutoff was set to 500 eV. The Brillouin zone integration was carried out with 2×3×1 Gamma point. The convergence thresholds for energy was set as 10^{-4} eV during ion relaxation and 10^{-6} eV during vibrational calculation, and the convergence thresholds for force was set as 0.05 eV • $Å^{-1}$.

Structures optimization: The six types N-doped graphene are optimized before attaching any molecules. The structural relaxation was performed until all forces were less than 0.05 eV/Å. The ground state structures of *CO and *COOH adsorbed on N-doped Graphene are determined by searching the lowest energy configurations on all active sites. The most stable configurations of *COOH is shown as Figure S11

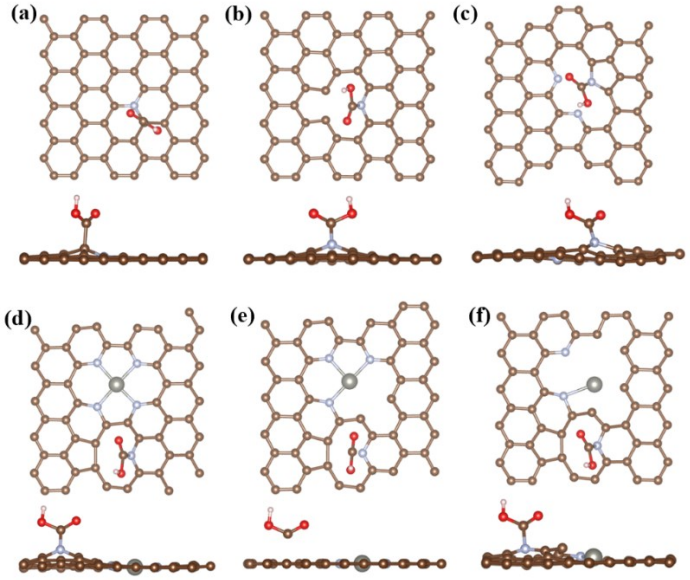

Figure S11 (a-f) The ground state structures *COOH adsorbed on Graphitic N, Pyridinic N, Pyrrolic N, Pyridinic N adjacent to Zn-N_4, Zn-N_3V and Zn-N_2V_2, where V stands for coordination vacancy. The grey, light blue, brown, red and white spheres are Ni, N, C, O and H atoms.

Free energy calculation: The free energy for each reactant is calculated as: $G = E_{DFT} + E_{ZPE} + \int_0^T CpdT - TS$. The E_{DFT} is the electronic energy calculated by DFT, and the E_{ZPE} is the zero point energy estimated within the harmonic approximation calculated by DFT. The $\int_0^T CpdT$ and TS are heat capacity and entropy at 298.15 K. The chemical potential of a pair of proton and electron can be calculated as a function of applied potential: $\mu(H^+)_+ \mu(e^-) = \frac{1}{2}\mu(H^2) - eU$, according to the

CHE model proposed by Nørskov et. Al[8]. Due to the PBE functional, the solvent effect for stabilizing *COOH and *CO was 0.25 and 0.10 eV, respectively. The correction to gas-phase CO was -0.51 eV[9, 10].

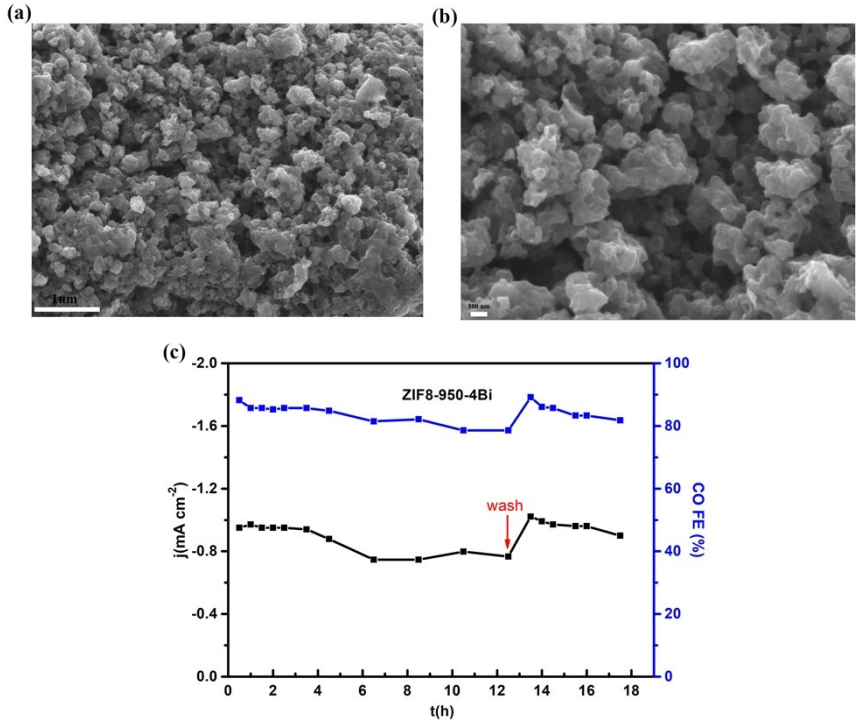

Figure S12. (a-b) SEM images of ZIF8-950-4Bi after electrolytic at -0.6 V vs for 18 h, (c) Stability of ZIF8-950-4Bi at -0.6 V vs. RHE in CO_2-saturated 0.5 M $KHCO_3$ solutions.

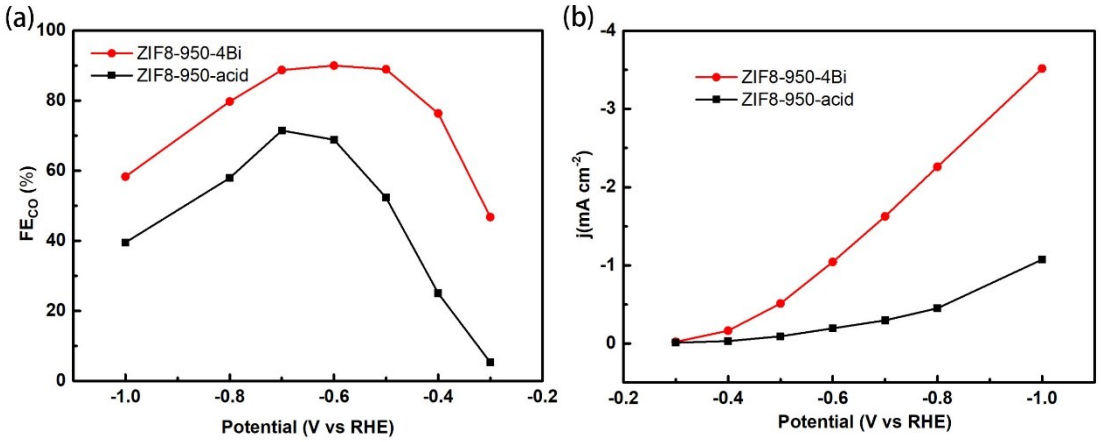

Figure S13. (a-b) the Faradaic efficiencies and current density for CO production at applied potentials on ZIF8-950-4Bi and ZIF8-950-acid.

Table S1 The ICP of Bi content for all samples.

Bi（Weight%）	ZIF8-950-Bi	ZIF8-950-2Bi	ZIF8-950-4Bi
ICP	0.07	0.04	0.04

Table S2 The EDS and XPS of Zn content for all samples.

Zn（Atomic%）	ZIF8-950	ZIF8-950-Bi	ZIF8-950-2Bi	ZIF8-950-4Bi
EDS	1.24	0.74	0.72	0.40
XPS	2.21	1.87	2.03	0.39

Table S3 The N content and kinds for all samples.

Type of N	ZIF8-950	ZIF8-950-Bi	ZIF8-950-2Bi	ZIF8-950-4Bi
Total N (%)	7.92	7.13	7.33	5.66
Pyridinic N (%)	2.24(28%)	1.85(26%)	2.09 (29%)	1.23 (22%)
Pyrrolic N (%)	1.71(22%)	1.87(26%)	1.77(24%)	1.61(28%)
Graphitic N (%)	2.50(31%)	2.39(34%)	2.33(31%)	2.11(38%)
Zn-N(%)	1.47(19%)	1.02(14%)	1.14(16%)	0.7(12%)

Table S4 The surface area and porous structure for the materials

Sample	S(m^2/g)	S_{mic}(m^2/g)	V_t(cm^3/g)	V_{mic}(cm^3/g)
ZIF8-950	910	751	0.89	0.40
ZIF8-950-Bi	862	689	0.70	0.36
ZIF8-950-2Bi	859	656	0.67	0.35
ZIF8-950-4Bi	785	437	0.82	0.24
ZIF8	1157	1066	1.08	0.56

References

1 G. Kresse and J. Furthmüller, *Physical Review B*, 1996, **54**, 11169-11186.
2 P. E. Blöchl, *Physical Review B*, 1994, **50**, 17953-17979.
3 J. P. Perdew, K. Burke and M. Ernzerhof, *Physical Review Letters*, 1996, **77**, 3865-3868.
4 J. P. Perdew, M. Ernzerhof and K. Burke, 1996, **105**, 9982-9985.
5 S. Grimme, *Wiley Interdisciplinary Reviews: Computational Molecular Science*, 2011, **1**, 211-228.
6 S. Grimme, *Journal of Computational Chemistry*, 2004, **25**, 1463-1473.
7 E. R. Johnson and A. D. Becke, *The Journal of Chemical Physics*, 2006, **124**, 174104.
8 A. A. Peterson, F. Abild-Pedersen, F. Studt, J. Rossmeisl and J. K. Norskov, *Energy & Environmental Science*, 2010, **3**, 1311-1315.
9 S. Liu, H. Yang, X. Huang, L. Liu, W. Cai, J. Gao, X. Li, T. Zhang, Y. Huang and B. Liu, *Advanced Functional Materials*, 2018, **28**.
10 J. Wu, M. Liu, P. P. Sharma, R. M. Yadav, L. Ma, Y. Yang, X. Zou, X. D. Zhou, R. Vajtai, B. I. Yakobson, J. Lou and P. M. Ajayan, *Nano Lett*, 2016, **16**, 466-470.